

Influence of confinement on the vibrational density of states and the Boson peak in a polymer glass

Tushar S. Jain and Juan J. de Pablo^{a)}

University of Wisconsin-Madison, Department of Chemical and Biological Engineering,
Madison, Wisconsin 53706

(Received 12 December 2003; accepted 3 February 2004)

We have performed a normal-mode analysis on a glass forming polymer system for bulk and free-standing film geometries prepared under identical conditions. It is found that for free-standing film glasses, the normal-mode spectrum exhibits significant differences from the bulk glass with the appearance of an additional low-frequency peak and a higher intensity at the Boson peak frequency. A detailed eigenvector analysis shows that the low-frequency peak corresponds to a shear-horizontal mode which is predicted by continuum theory. The peak at higher frequency (Boson peak) corresponds to motions that are correlated over a length scale of approximately twice the interaction site diameter. These observations shed some light on the microscopic dynamics of glass formers, and help explain decreasing fragility that arises with decreasing thickness in thin films. © 2004 American Institute of Physics. [DOI: 10.1063/1.1689952]

I. INTRODUCTION

Glassy materials are of interest from both a fundamental and a technological perspective. Unfortunately, the diversity of behavior observed in these systems is not satisfactorily explained either by phenomenological theories or from first principles.^{1,2} Over the last decade, significant efforts have been devoted to the study of glasses under confinement. Part of the premise behind such efforts has been that introducing a specified directionality could provide insights of how cooperative processes arise in glasses. The glass transition temperature T_g exhibits finite-size effects in systems with critical dimensions on the order of tens of nanometers. For example, in the case of supported thin polymer films, T_g can either increase or decrease with decreasing thickness depending on the nature of the substrate.^{3,4} In the case of thin free-standing polymer films, T_g generally decreases with decreasing thickness,⁵ with reductions of the order of 60 K for free-standing films of thickness 30 nm (for polystyrene). Since the structural and mechanical properties degrade rapidly above T_g , this decrease (or increase) often dictates the temperature range of applicability of these materials. A fundamental understanding of the mechanisms that govern the glass transition in confined geometries would facilitate design of better polymers for thin film applications.

Several models^{6–9} have been proposed to explain the shift of T_g in confined systems. The model of Mattsson *et al.*⁶ explains the reduction of T_g in low molecular weight polystyrene films by introducing the concept of a surface layer, with lower T_g , and a bulk portion with a bulk T_g . It has also been proposed that the dynamics in thin films are dominated by a “sliding motion” mechanism which leads to the observed reduction of T_g .⁷ Using scaling arguments, an expression for T_g has been derived that, in agreement with experiment, predicts a linear decrease of T_g with decreasing

thickness for large molecular weights. Recently, Herminghaus⁹ has proposed a model based on the coupling of capillary waves at the surface of a polymer film to the dynamics of the films. The model is able to predict the depression of T_g in free-standing films by using the Young's modulus as a fitting parameter. Several literature studies have used molecular simulations^{2,10–14} to study thin polymer films and have observed higher rates of relaxation and greater mobility at interfaces, thereby lending credence to the existence of a surface mobile layer.

An analysis in terms of the potential energy landscape (PEL)^{15,16} provides a useful framework for understanding and quantifying the thermodynamic and dynamic changes observed in glasses. In this approach, the PEL is partitioned into energy basins connected by saddle points that lead the system from one basin to another. One view of the dynamics in glassy systems assumes that short-time (microscopic) relaxation occurs due to intrabasin motions, and that long-time relaxation occurs via infrequent jumps over saddle points into neighboring basins. The thermodynamics of glassy systems can also be described in terms of the statistical properties of the landscape.¹⁷ Such an approach has also been recently extended to the study of thin films.¹⁸ In this work, we have focused our attention on the nature of the normal modes and the Boson peak at potential-energy minima of a glassy polymer in the bulk and in a thin film. The use of thin films gives us a reference for studying the dependence of these modes with respect to a particular direction (e.g., normal to the film) which is absent in the case of bulk systems. We have carefully analyzed the influence of confinement on the underlying PEL of these systems using the normal mode formalism. Furthermore, we have resolved the particle motions in the normal modes with the aim of understanding the different dynamics, if any, and their origin in these confined systems.

^{a)} Author to whom all correspondence should be addressed.

II. THEORY AND SIMULATION DETAILS

The potential energy $\Phi(\mathbf{x})$, of a system of N particles close to its minimum \mathbf{x}_0 can be expressed through a second-order Taylor series expansion as follows:

$$\Phi(\mathbf{x}) = \Phi(\mathbf{x}_0) + \mathbf{F} \cdot (\mathbf{x} - \mathbf{x}_0) + \frac{1}{2} (\mathbf{x} - \mathbf{x}_0) \cdot \mathbf{H} \cdot (\mathbf{x} - \mathbf{x}_0) + \dots, \quad (1)$$

where \mathbf{x} is the vector of particle positions, \mathbf{F} is the force vector, and \mathbf{H} is the Hessian matrix,

$$F_{i\alpha} = \left. \frac{\partial \Phi}{\partial r_{i\alpha}} \right|_{\mathbf{x}=\mathbf{x}_0}$$

$$H_{i\alpha, j\beta} = \left. \frac{\partial^2 \Phi}{\partial r_{i\alpha} \partial r_{j\beta}} \right|_{\mathbf{x}=\mathbf{x}_0}$$

where $i, j = 1, \dots, N$ and $\alpha, \beta = x, y, z$. At a potential-energy minimum, $\mathbf{F} = 0$. A diagonalization of the Hessian is performed to obtain the $3N$ eigenvalues and corresponding eigenvectors. Each eigenvalue ω_k is a normal-mode frequency and its associated eigenvector \mathbf{Q}_k is a normal-mode coordinate. The value of ω_k gives the curvature of the PEL as the system moves along the normal mode \mathbf{Q}_k . Each eigenvector \mathbf{Q}_k has length $3N$, which can be thought of as N displacement vectors \mathbf{q}_i acting on the particles in the system,

$$\mathbf{Q}_k = [\mathbf{q}_1, \dots, \mathbf{q}_N]_k,$$

where $k = 1, \dots, 3N$. These particle vectors give the direction and displacement of the particles in a particular eigenmode k .

Based on the correlation of these displacement vectors between neighboring particles in a particular mode, we can establish whether the mode has a long-range or short-range character. To quantify this, an angle θ_{ij} is defined between the displacement vectors \mathbf{q}_i and \mathbf{q}_j of particles i and j in a particular mode. The correlation of θ_{ij} as a function of distance r_{ij} between the particles is examined using the following order parameter:

$$P(\theta_{ij}) = \frac{3\langle \cos^2 \theta_{ij} \rangle - 1}{2}. \quad (2)$$

The brackets denote an average over the displacement vectors on the particles in a particular mode. For free-standing films, the orientation of these modes with respect to the direction \mathbf{z} normal to the film is studied by plotting $P(\theta_z)$ for the angle between the particle displacement vectors and \mathbf{z} . This correlation is further studied as a function of distance from the free surface to compare the direction of motion at the film surface and in the bulk. In order to distinguish between modes dominated either by motions at the surface or the bulk, we analyze the average magnitude of the displacement on the particles as a function of position in the film.

The model employed in this work consists of interaction sites on a chain having a diameter σ and characteristic energy ϵ . Nonbonded sites interact through the 6-12 Lennard-Jones potential, and bonded sites interact through a harmonic potential,

$$U_{ij}^{\text{nb}} = 4\epsilon \left[\left(\frac{\sigma}{r_{ij}} \right)^{12} - \left(\frac{\sigma}{r_{ij}} \right)^6 \right], \quad (3)$$

$$U_{ij}^b = \frac{k_h}{2} (r_{ij} - \sigma)^2, \quad (4)$$

where $k_h = 2000\epsilon/\sigma^2$. These parameters were chosen to prevent crystallization and facilitate trapping of the system in an amorphous glassy state. The chains used in this work have length $L = 32$. All the results are reported in reduced variables, i.e., temperature $T^* = kT/\epsilon$ and density $\rho^* = N\sigma^3/V$.

Four systems are considered in this work; a bulk glass and three free-standing film glasses of thicknesses 24σ , 12σ , and 10σ , respectively. Equilibration of these systems was carried out using advanced Monte Carlo moves such as reptation, end-configurational bias, and end-bridging and molecular dynamics in the NPT ensemble at a pressure $P^* = 0.0$. The system was first equilibrated at $T^* = 1.2$, which is well above the estimated glass transition temperature. The temperature was then reduced in steps of 0.1 until $T^* = 0.6$ and then in steps of 0.05.

A glass transition temperature T_g , was identified for the bulk system as the point where the density vs temperature curve changes slope. This glass transition temperature was determined to be $T_g^b = 0.40$. For the thin films, the glass transition temperature was similarly determined from the temperature dependence of the film thickness. A decrease in T_g with film thickness is observed, which is consistent with the experimental measurements on thin free-standing films.

In order to perform a normal-mode analysis, we periodically saved configurations over simulation runs of the order of 50 million time steps and minimized the potential energy using a conjugate gradient algorithm.¹⁹ A key point to note in this procedure is that, for a free-standing film, the thickness and therefore the density in the center of the film changes during the minimization. Therefore, in the case of minimizations of bulk configurations, we treated the volume as an additional variable in the minimization procedure. Therefore, at the minima obtained, the derivative of the potential energy is zero with respect to the particle positions and the changes in the simulation box volume. The pressure calculated according to the virial equation was approximately zero at the minima. The densities obtained in the bulk of the thin films and the bulk glass were the same (within statistical error) at the end of the minimization procedure. The results presented are for configurations sampled at $T^* = 0.45$, which is above the glass transition temperature. However, the density changes during the minimization and the final density of the minimized configurations ($\rho^* \approx 1.05$) was well into the glassy regime. The normal modes obtained here are characteristic of those close to the minima in the hyperquenched glasses.

III. RESULTS

In Fig. 1, we have plotted the normalized distribution of eigenfrequencies $g(\omega)$, obtained from \mathbf{H} . A peak is observed in the high-frequency regime [Fig. 1(b)], corresponding to the spring constant k_h of the bonded potential. Within statistical error, the spectrum is identical for all systems at high

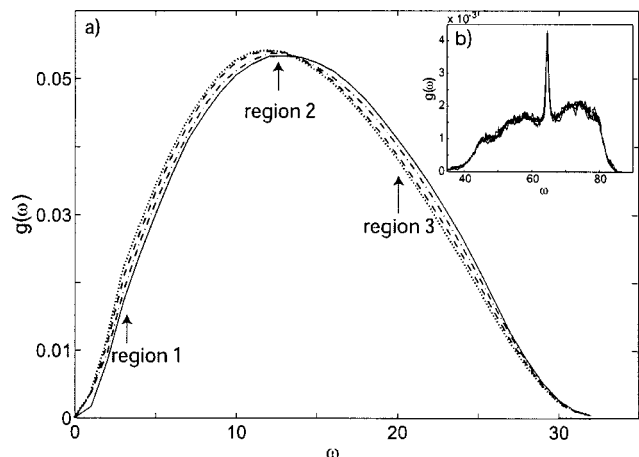


FIG. 1. (a) The lower portion of the vibrational density of states $g(\omega)$, for the polymer glass (dotted line: 10σ ; dashed line: 12σ ; dash-dot line: 24σ ; and solid line: bulk). (b) The vibrational density of states for the higher frequencies.

frequencies ($\omega > 35$). In order to locate the Boson peak for the systems considered here, we have plotted $g(\omega)/\omega^2$ in Fig. 2. The thin films exhibit a prominent peak at low frequencies, and a plateau region at higher ω , corresponding to the peak frequency observed in the bulk glass (Boson peak). An investigation of the eigenvectors corresponding to the lower frequency peak of the thin films reveals that the displacement in these modes is polarized in the horizontal direction, and decreases smoothly from a finite value at the free interface to zero at the center of the film. These modes are predicted by continuum mechanics,²⁰ and are referred to as shear-horizontal modes. Continuum mechanics also predicts that the frequency of these modes is inversely proportional to the film thickness. Figure 2(b) shows that this prediction is consistent with the results of our simulations.

In the region of the peak at higher frequency ($\omega \approx 2.5$), one can observe that the intensity of the Boson peak increases with decreasing thickness. For convenience, we have

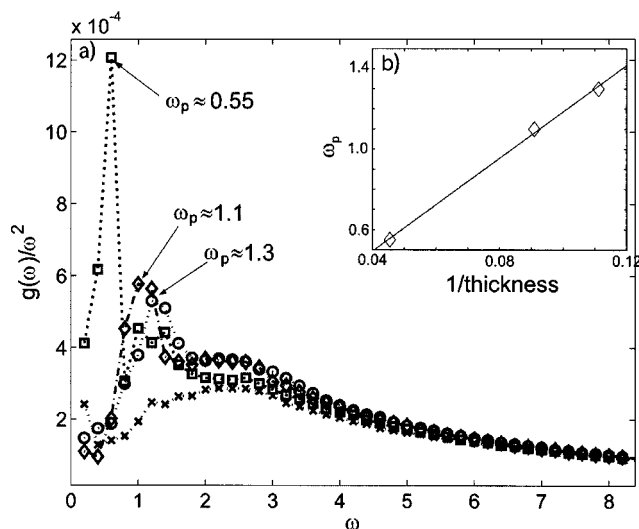


FIG. 2. (a) Influence of confinement on the Boson peak (\circ : 10σ ; \diamond : 12σ ; \square : 24σ ; and \times : bulk). (b) Test of the scaling prediction from continuum mechanics for shear-horizontal modes.

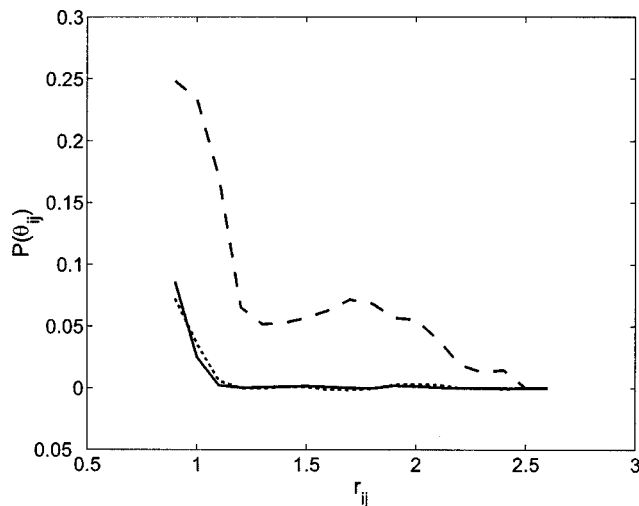


FIG. 3. Correlation of the displacement vectors on the particles in the different modes. The dashed line, solid line, and dotted line denote regions 1, 2, and 3, respectively.

divided the spectrum into three regions numbered from 1 to 3 (Fig. 1). In order to characterize the nature of this shift, we have analyzed the eigenvectors corresponding to these three regions in detail, in small domains of width $\Delta\omega = 1$, centered at the arrows.

Figure 3 shows $P(\theta_{ij})$ for the correlation of the directions of the particle displacement vectors as a function of distance between the particles for the film of thickness 12σ . The correlation decays to zero after approximately one site diameter for the eigenvectors in regions 2 and 3. However, in region 1, the correlation decays over a length slightly greater than 2σ . This suggests that the modes in region 1 are more cooperative in nature than those in the other regions of the frequency spectrum. Similar results are also obtained for the bulk system (not shown).

Figure 4 shows $P(\theta_z)$ as a function of position for the film of thickness 12σ . A clear distinction can be observed for modes belonging to different regions of the spectrum. In re-

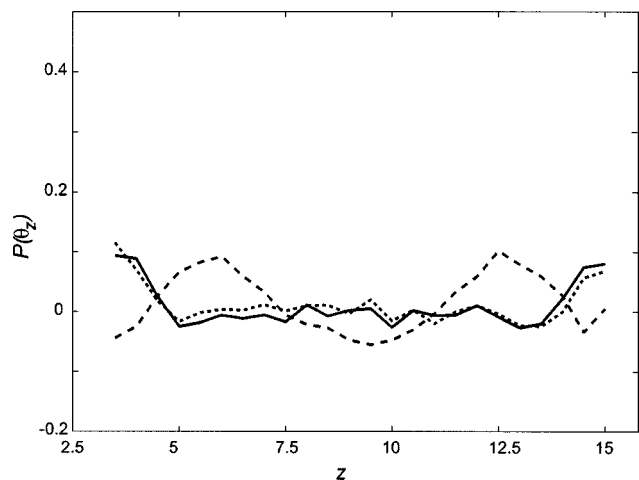


FIG. 4. Correlation of the displacement vectors on the particles with the film normal in the different modes as a function of position in the film. The dashed line, solid line, and dotted line denote regions 1, 2, and 3, respectively.

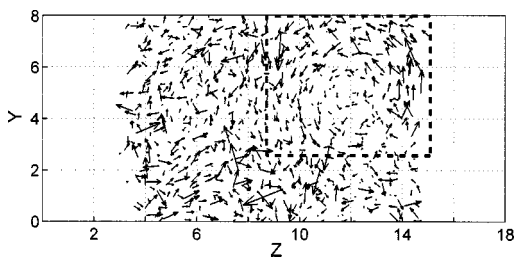


FIG. 5. Eigenvector for a mode of frequency $\omega=2.21$, belonging to region 1. The arrows indicate the direction and magnitude of the displacement field on the interaction sites which are not shown for clarity. The dashed box encloses a region that shows a clear presence of a displacement field representing a vortex.

regions 2 and 3, we can see that interfacial particles have a tendency to move normal to the film, whereas there is no distinct direction dependence in the center region of the film. The lower frequency region (region 1) exhibits motion that shows well defined oscillations over the entire thickness of the film. A closer look at the eigenvectors corresponding to the low frequencies reveals that these modes involve the presence of vortices in the film (Fig. 5). In order to characterize the contribution of the film interface and the bulk in a particular mode, we have analyzed the magnitude of the displacement on the particles as a function of position in the film. Figure 6 shows d/d_b (the average magnitude of displacement normalized by the bulk displacement) in a particular mode for the three regions. We find that the modes in region 3 are dominated by motions in the bulk of the film. However, in region 1, the interfacial particles exhibit larger displacements compared to the bulk particles. The results are qualitatively the same for the films of thickness 10σ and 24σ . As expected, in the case of the bulk system (not shown), the displacement vectors have no direction or position dependence.

IV. CONCLUSIONS

We have characterized the normal modes for bulk and free-standing film polymer glasses, and find a systematic influence of the presence of free interfaces on the minima of these systems. There is a distinct separation between the

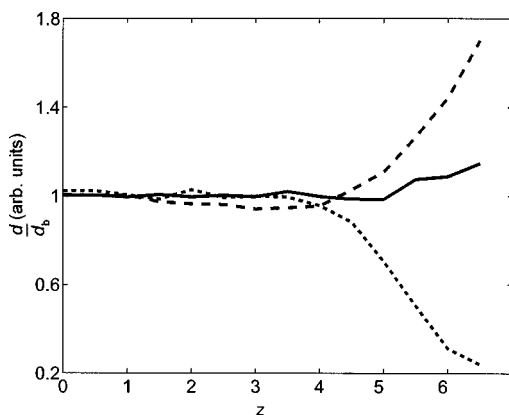


FIG. 6. Magnitude of the displacement vector d , on the particles in the different modes as a function of position in the film. The dashed line, solid line, and dotted line denote regions 1, 2, and 3, respectively.

modes that correspond to motion at the interface and motion in the center of the film. The fraction of low-frequency modes and the intensity at the Boson peak frequency increase with confinement. An enhancement of the Boson peak has also been observed experimentally in mineral glasses for hyperquenched samples when compared to their annealed counterparts.²¹ In our study, the minimized bulk and film systems can be considered to be hyperquenched glasses. However, the differences between the film and bulk glasses arise solely on account of the confinement since all the configurations in our study have been prepared using the same protocol. We find that the thin-film glass *appears* to be hyperquenched to a greater degree than the bulk. The change in the intensity of the Boson peak with thickness is also consistent with empirical observations that suggest a decreasing fragility with an increasing strength of the Boson peak.²² Extending this observation to free-standing films would imply a decrease in fragility in thin films compared to the bulk system. Such a decrease has been alluded to in previous simulations of shorter chains in the continuum¹² and longer chains on a lattice,¹³ and has been observed experimentally in intercalated polymer films.²³ A higher probability of low-frequency modes can have important implications for glassy dynamics; a greater number of directions with lower curvature could facilitate the escape from a basin and rationalize the observed depression of T_g . Furthermore, in both the bulk and thin-film geometries, these modes correspond to motions that are correlated over larger length scales than other modes. Cooperative processes are believed to dominate the relaxation events in both model atomic and polymer glasses;^{24–27} a higher fraction of these modes is likely to be responsible for the accelerated relaxation of free-standing films. Indeed, it has been observed in soft-sphere glasses that the cooperative motions exhibit a significant degree of overlap with the low-frequency vibrations.^{28,29} For the films, the physical picture of the low-frequency modes is that they represent an increased tendency for motion near the film interface. Our results show that even for configurations that are in the vicinity of potential-energy minima (well into the glassy regime, as opposed to above or approaching T_g), there is a clear signature for the presence of a mobile surface layer in glassy films. It would be interesting to calculate the transition states and the energy barriers between minima using eigenvector-following algorithms,^{30–33} and observe the actual structural transitions that lead to barrier crossings and the height of the energy barriers. Calculations of this nature have been performed for model systems in the bulk or in small clusters^{34–37} and have elucidated the mechanisms involved in such transitions. We are currently investigating this issue and results will be presented in a future publication.

ACKNOWLEDGMENTS

This work is supported by a NIRT grant from the National Science Foundation (CTS-0210588) and by the Semiconductor Research Corporation (2002-MJ-985).

¹J. Forrest, Eur. Phys. J. E **8**, 261 (2002).

²K. Binder, J. Baschnagel, and W. Paul, Prog. Polym. Sci. **28**, 115 (2003).

³D. Fryer *et al.*, Macromolecules **34**, 5627 (2001).

- ⁴J. L. Keddie, R. A. L. Jones, and R. Cory, *Europhys. Lett.* **27**, 59 (1994).
⁵K. Dalnoki-Veress *et al.*, *Phys. Rev. E* **63**, 031801 (2001).
⁶J. Mattsson, J. Forrest, and L. Börjesson, *Phys. Rev. E* **62**, 5187 (2000).
⁷P. de Gennes, *Eur. Phys. J. E* **2**, 201 (2000).
⁸D. Long and F. Lequeux, *Eur. Phys. J. E* **4**, 371 (2001).
⁹S. Herminghaus, *Eur. Phys. J. E* **8**, 237 (2002).
¹⁰K. F. Mansfield and D. N. Theodorou, *Macromolecules* **24**, 6283 (1991).
¹¹W. Xu and W. L. Mattice, *J. Chem. Phys.* **118**, 5241 (2003).
¹²J. A. Torres, P. F. Nealey, and J. J. de Pablo, *Phys. Rev. Lett.* **85**, 3221 (2000).
¹³T. S. Jain and J. J. de Pablo, *Macromolecules* **35**, 2167 (2002).
¹⁴P. Doruker and W. L. Mattice, *J. Phys. Chem. B* **103**, 173 (1999).
¹⁵F. H. Stillinger and T. A. Weber, *Phys. Rev. A* **28**, 2408 (1983).
¹⁶M. Goldstein, *J. Chem. Phys.* **51**, 3728 (1969).
¹⁷S. Sastry, *Nature (London)* **409**, 164 (2001).
¹⁸T. M. Truskett and V. Ganesan, *J. Chem. Phys.* **119**, 1897 (2003).
¹⁹W. H. Press, S. A. Teukolsky, W. T. Vetterling and B. P. Flannery, *Numerical Recipes in C* (Cambridge, New York, 1988).
²⁰B. A. Auld, *Acoustic Fields and Waves in Solids* (Kreiger, Malabar, 1990).
²¹C. A. Angell *et al.*, *J. Phys.: Condens. Matter* **15**, S1051 (2003).
²²C. A. Angell *et al.*, *J. Appl. Phys.* **88**, 3113 (2000).
²³S. H. Anastasiadis *et al.*, *Phys. Rev. Lett.* **84**, 915 (1999).
²⁴T. Schröder, S. Sastry, J. Dyre, and S. Glotzer, *J. Chem. Phys.* **112**, 9834 (2000).
²⁵C. Donati *et al.*, *Phys. Rev. Lett.* **80**, 2338 (1998).
²⁶Y. Gebremichael, T. Schröder, F. Starr, and S. Glotzer, *Phys. Rev. E* **64**, 051503 (2003).
²⁷C. Bennemann, C. Donati, J. Baschnagel, and S. Glotzer, *Nature (London)* **399**, 246 (1999).
²⁸H. Schober and C. Oligschleger, *Phys. Rev. B* **53**, 11 469 (1995).
²⁹H. Schober and B. B. Laird, *Phys. Rev. B* **44**, 6746 (1991).
³⁰J. Baker, *J. Comput. Chem.* **7**, 385 (1986).
³¹C. H. Cerjan and W. H. Miller, *J. Chem. Phys.* **75**, 2800 (1981).
³²J. Simons, P. Jorgensen, H. Taylor, and J. Ozment, *J. Phys. Chem.* **87**, 2745 (1983).
³³G. Henkelman and H. Jónsson, *J. Chem. Phys.* **111**, 7010 (1999).
³⁴T. Middleton and D. Wales, *Phys. Rev. B* **64**, 024205 (2001).
³⁵J. Doye and D. Wales, *J. Chem. Phys.* **116**, 3777 (2002).
³⁶R. Malek and N. Mousseau, *Phys. Rev. E* **62**, 7723 (2000).
³⁷N. P. Kopsias and D. N. Theodorou, *J. Chem. Phys.* **109**, 8573 (1998).